

# Design and Development of Quasi-Monoenergetic Neutron Source using the Inverse Kinematics of (p,n) Reaction

Y. Matsuoka, Y. Watanabe<sup>a)</sup>, S. Hachiya, H. Nakamura, Y. Tanaka  
N. Ikeda\* and K. Sagara\*

*Department of Advanced Energy Engineering and Science, Kyushu University,  
Kasuga-kouen, Kasuga, Fukuoka-ken 816-8580*

*\*Department of Physics, Kyushu University, Hakozaki, Higashi-ku, Fukuoka 812-0053*

<sup>a)</sup> e-mail: watanabe@aees.kyushu-u.ac.jp

We have started to develop a new quasi-monoenergetic neutron source using the inverse kinematics of (p,n) reaction at Kyushu University Tandem Laboratory. A preliminary experiment was performed for a neutron source using the  $^1\text{H}(^{13}\text{C},\text{n})^{13}\text{N}$  reaction at an incident energy of 59.3 MeV. It was experimentally observed that monoenergetic neutrons with about 7 MeV were produced at  $0^\circ$  in the laboratory system and the produced neutrons were collimated to a forward cone restricted by the kinematics.

## 1. Introduction

There are various types of accelerator-based monoenergetic neutron sources that are widely used in basic science and applications. In the energy region covered by tandem Van de Graaf accelerators, light-ion induced reactions on light element targets, such as the  $\text{D}(\text{d},\text{n})^3\text{He}$ ,  $\text{T}(\text{d},\text{n})^4\text{He}$ ,  $\text{T}(\text{p},\text{n})^3\text{He}$  and  $^7\text{Li}(\text{p},\text{n})^7\text{Be}$  reactions, are popular as the nuclear reactions to produce monoenergetic neutrons. However, these reactions cannot produce the real monoenergetic neutrons in the energy region between 8 and 14 MeV because of the breakup of the projectile and/or the target nucleus. Therefore, only few neutron cross section data is now available in this “gap” region, whereas the data in this energy region is required in several applications, e.g., the development of D-T fusion reactors.

Recently, new types of monoenergetic neutron sources with heavy ion (HI) beams have been proposed as one of the candidates to fill in the “gap” region and the feasibility has so far been investigated.[1,2,3] A neutron source with the  $^1\text{H}(^{11}\text{B},\text{n})^{11}\text{C}$  reaction were practically used for measurements of some activation cross sections in the 9 to 13 MeV region [4] and the usefulness was demonstrated.

Under these circumstances, we have started the development of a monoenergetic neutron source in this “gap” region by using the  $^1\text{H}(\text{HI},\text{n})$  reaction at Kyushu University Tandem Laboratory (KUTL). The  $^1\text{H}(^{13}\text{C},\text{n})^{13}\text{N}$  reaction was chosen as a suitable candidate for KUTL from consideration about the performance of accelerator and its feasibility test has been performed.

## 2. The $^1\text{H}(\text{HI},\text{n})$ neutron source

Characteristic features of the  $^1\text{H}(\text{HI},\text{n})$  neutron source are summarized as follows:

- 1) In an endothermic reaction, the produced neutrons are emitted at angles smaller than  $\theta_{\text{max}}$  defined by two-body kinematics, that is, the neutrons are “kinematically collimated” into a forward cone. This situation is schematically illustrated in Fig. 1, and a calculation of the kinematics for the  $^1\text{H}(^{13}\text{C},\text{n})^{13}\text{N}$  reaction is shown in Fig. 2.

By this collimation, the shielding design of neutron facilities is expected to become easier.

- 2) The  $^1\text{H}(\text{HI},\text{n})$  cross section at  $0^\circ$  in the laboratory system is enhanced strongly by the compression into the forward cone, which leads to large neutron yield at  $0^\circ$ .
- 3) The emitted neutrons at one angle have two energies as shown in Figs. 1 and 2. The neutrons with higher energy are called “primary” neutrons and those with lower energy are called “satellite” neutrons. However, the energy and yield of the “satellite” neutrons is considerably smaller than the “primary” neutrons under most experimental conditions.
- 4) The smaller backgrounds of neutrons and  $\gamma$  rays from the beam stopper can be expected because the heavy projectiles have much higher Coulomb barrier than protons and deuterons.

### 3. Design of the neutron source and simulation of neutron production

As a hydrogen target for the  $^1\text{H}(^{13}\text{C},\text{n})^{13}\text{N}$  reaction, we have chosen a gas target. A schematic drawing of the fabricated gas target is shown in Fig. 3. It is made of stainless steel and has the effective size of 30 mm long and 33 mm in diameter. The entrance window is made of tantalum foil of 3  $\mu\text{m}$  in thickness and 12 mm in diameter, and a 0.2 mm thick tantalum disk is used as the beam stopper so that associated backgrounds of neutrons and  $\gamma$  rays may be reduced as much as possible by using high Z materials. The escape of the electrons produced by beam bombardment on the entrance window is suppressed by the permanent magnets.

In the design of the neutron source, we have estimated neutron yields at  $0^\circ$  in laboratory system using a modified version of the simulation code [5] developed for  $^1\text{H}(^{11}\text{B},\text{n})^{11}\text{C}$  neutron source. Since there is no available cross section data of the  $^1\text{H}(^{13}\text{C},\text{n})^{13}\text{N}$  reaction, we used the cross sections derived from the  $^{13}\text{C}(\text{p},\text{n})^{13}\text{N}$  cross sections[6] in terms of the inverse kinematics. The calculated result for an incident energy of 58.2 MeV is shown in Fig. 4. The pressure of  $\text{H}_2$  gas was taken to be 1 atm. One can see two peaks that correspond to two neutron components. It is found that the yield of the “primary” neutrons (about 7 MeV) is much larger than the “satellite” neutrons (about 1 MeV).

## 4. Preliminary experiment and results

### 4.1. Experimental procedure

The first test experiment was carried out using 59.3 MeV  $^{13}\text{C}^{6+}$  beam. The experimental setup is shown in Fig. 5. The average beam current was about 40 enA. The pressure of  $\text{H}_2$  gas in the gas cell target was 2 atm. The neutron yields were measured at angles,  $0^\circ$ ,  $10^\circ$ ,  $20^\circ$  and  $30^\circ$ , by using an active radiator proton recoil counter telescope (ARPRT)[7] which was placed 20 cm far from the center of the gas cell target.

### 4.2. Neutron yield at $0^\circ$

The recoil proton spectrum at  $0^\circ$  measured by ARPRT is shown in Fig. 6. The “satellite” neutrons shown in Fig. 4 could not be detected in this experiment, because the threshold energy of ARPRT was about 2 MeV. The experimental yield of 7.2 MeV neutrons for emission at  $0^\circ$  was  $(1.58 \pm 0.06) \times 10^7$  [n/sr/ $\mu\text{C}$ ]. This value was about 2.5 times smaller than the result estimated from the number of incident  $^{13}\text{C}$  ions, the pressure of  $\text{H}_2$  gas and the cross section of the  $^{13}\text{C}(\text{p},\text{n})^{13}\text{N}$  reaction[6]. One of the reasons may be due to the  $^{13}\text{C}(\text{p},\text{n})^{13}\text{N}$  cross section used, because the experimental values [6,8,9] in the energy region of interest are scattered within a factor of about two.

### 4.3. Angular distributions

In Fig. 7, the measured angular distribution of produced neutrons is compared with the two calculated results of  ${}^1\text{H}({}^{13}\text{C},\text{n}){}^{13}\text{N}$  and  $\text{D}(\text{d},\text{n}){}^3\text{He}$  neutron sources. Each angular distribution is normalized to each value at  $0^\circ$ . The experimental yield shows remarkable reduction at  $30^\circ$ . And, this trend is similar to the simulation result given by the solid line. Thus, it was experimentally confirmed that the neutrons produced by the  ${}^1\text{H}({}^{13}\text{C},\text{n}){}^{13}\text{N}$  reaction are emitted within the forward cone restricted by the kinematics. As shown in Fig. 7, however, a small fraction of neutrons are observed even at  $30^\circ$  over the kinematically allowed angle. The reason may be due partly to the reactions on some impurities in the  $\text{H}_2$  gas cell target, such as  $\text{H}_2\text{O}$  and/or air.

## 5. Summary

We have investigated the properties of the  ${}^1\text{H}({}^{13}\text{C},\text{n}){}^{13}\text{N}$  neutron source at KUTL. The preliminary experiment with 59.3 MeV  ${}^{13}\text{C}^{6+}$  beam showed that the  ${}^1\text{H}({}^{13}\text{C},\text{n}){}^{13}\text{N}$  reaction can produce the “kinematically collimated” monoenergetic neutrons with 7.2 MeV at  $0^\circ$ . The present work is in the first stage toward the completion of the monoenergetic neutron source using the  ${}^1\text{H}({}^{13}\text{C},\text{n}){}^{13}\text{N}$  reaction at KUTL. In the future, further optimization of the design will be necessary for the enhancement of neutron yields and the reduction of backgrounds in order to satisfy several requirements for practical use.

## References

- [1] M. Drogg.: Nucl. Sci. Eng. **106**, 279 (1990)
- [2] S. Chiba et al.: Nucl. Inst. Meth. **A281**, 581 (1989)
- [3] K. Hasegawa et al., Proc. 11<sup>th</sup> Int. Conf. Cyclotrons and Their Applications, Oct. 20-24, 1987, Tokyo, Japan, 642 (1987)
- [4] Y. Ikeda et al., Proc. of Int. Conf. on Nucl. Data for Sci. and Tech., May. 13-17, 1991, Julich, 294 (1992)
- [5] S. Meigo.: JAERI M-94-019, 243 (1994)
- [6] P. Dagley, et al.: Nucl. Phys. **24**, 353 (1961).
- [7] S. Hachiya.: Master thesis, Kyushu Univ., unpublished (1999).
- [8] O. Dietzsch.: Nucl. Phys. **85**, 689 (1966).
- [9] J. Gibbons, et al.: Phys. Rev. **114**, 571 (1959).

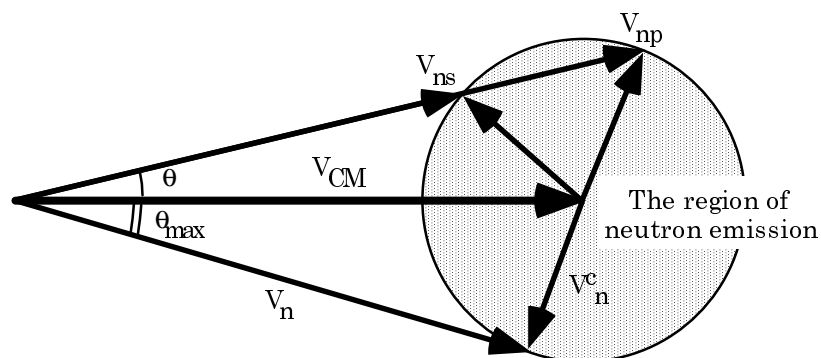


Fig. 1: Schematic diagram of two-body kinematics for the  ${}^1\text{H}(\text{HI},\text{n})$  reaction under the condition  $V_{\text{CM}} > V_{\text{n}}^{\text{c}}$ , where  $V_{\text{CM}}$  denotes the velocity of the CM, and  $V_{\text{n}}^{\text{c}}$  that of the produced neutron in the CM.  $\theta_{\text{max}}$  is the maximum angle of neutron production in laboratory system.

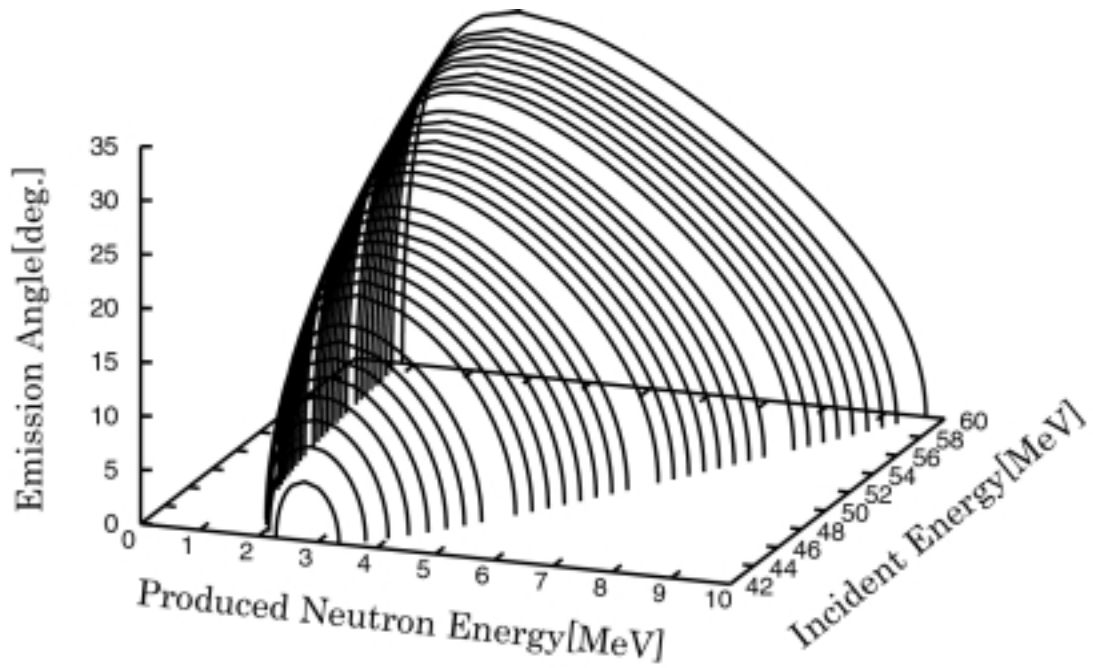


Fig.2: Neutron emission angle as a function of neutron emission energy and incident heavy-ion energy calculated using the two-body kinematics for the  ${}^1\text{H}({}^{13}\text{C},n){}^{13}\text{N}$  reaction.

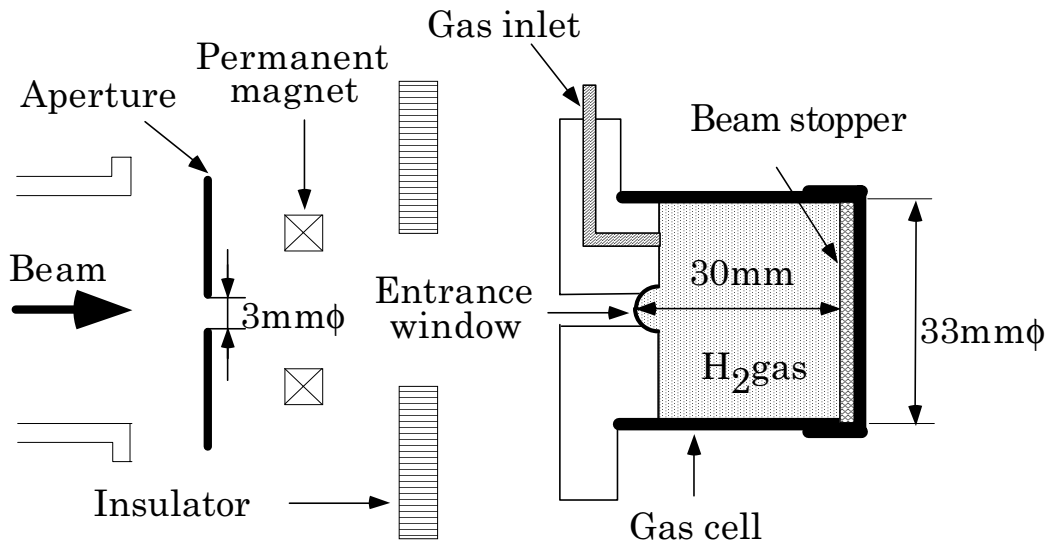


Fig. 3: Schematic drawing of the  $\text{H}_2$  gas cell target

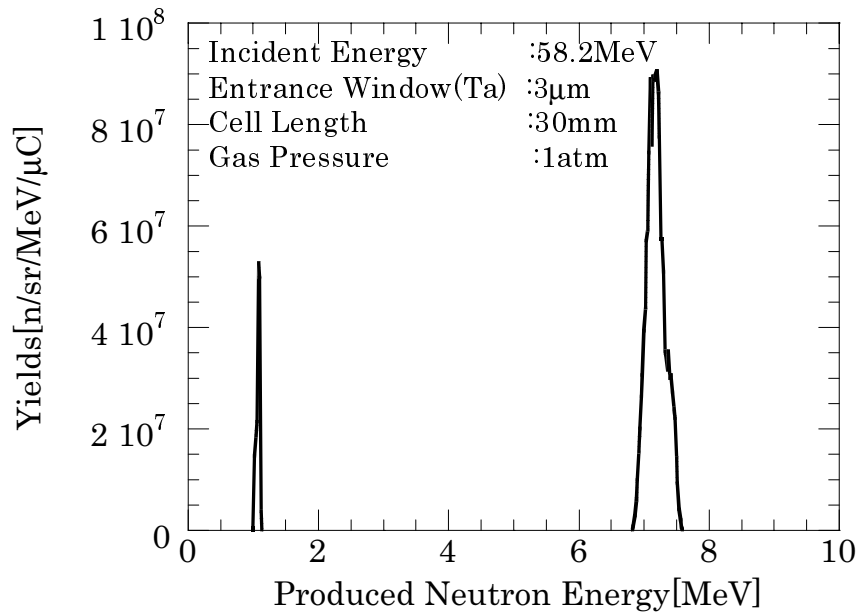


Fig. 4: Calculated spectrum of neutrons produced by the  $^1\text{H}(^{13}\text{C},n)^{13}\text{N}$  reaction at 58.2 MeV in the  $0^\circ$  direction.

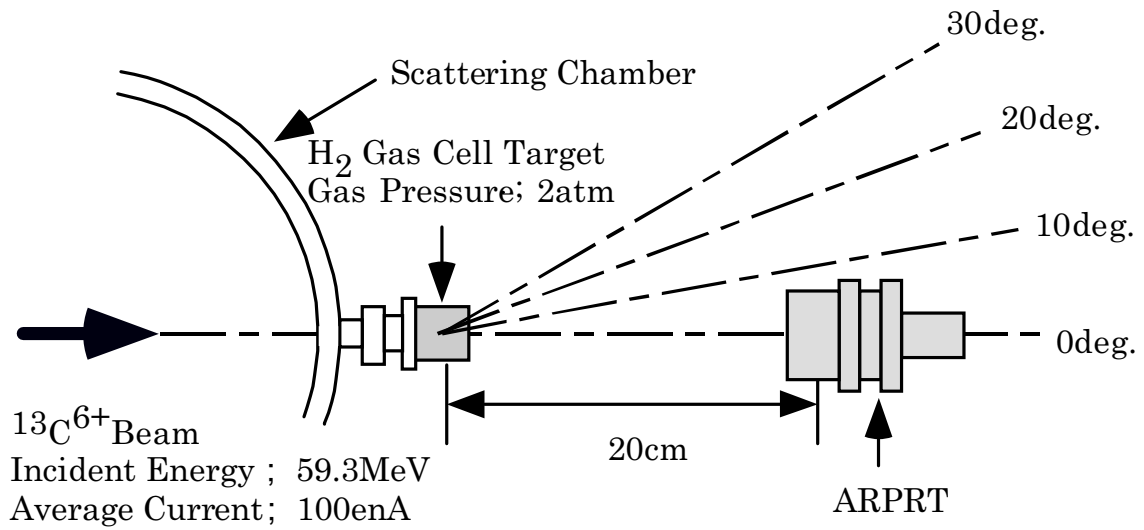


Fig. 5: Experimental setup at KUTL

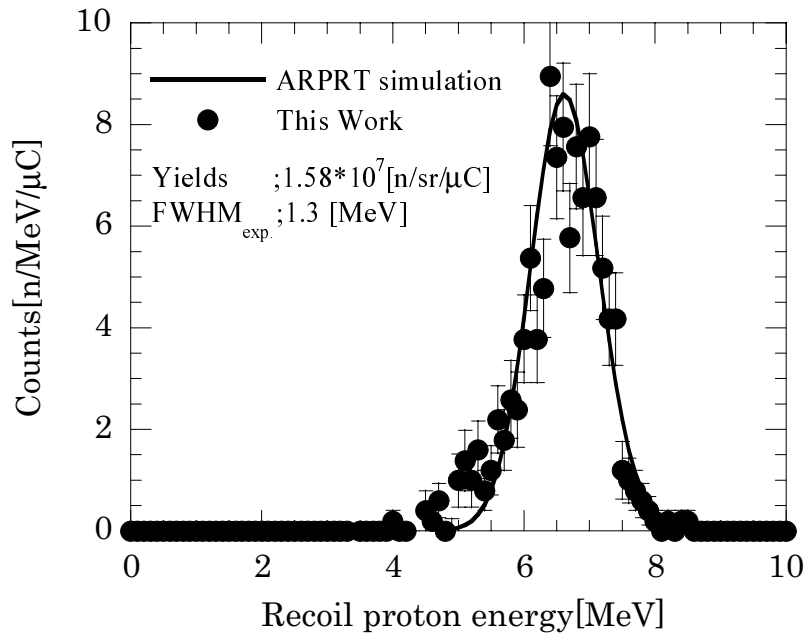


Fig. 6: Measured proton spectrum for 7.2 MeV neutrons produced by the  ${}^1\text{H}({}^{13}\text{C},\text{n}){}^{13}\text{N}$  reaction using ARPRT. The solid line represents the calculated response of ARPRT.

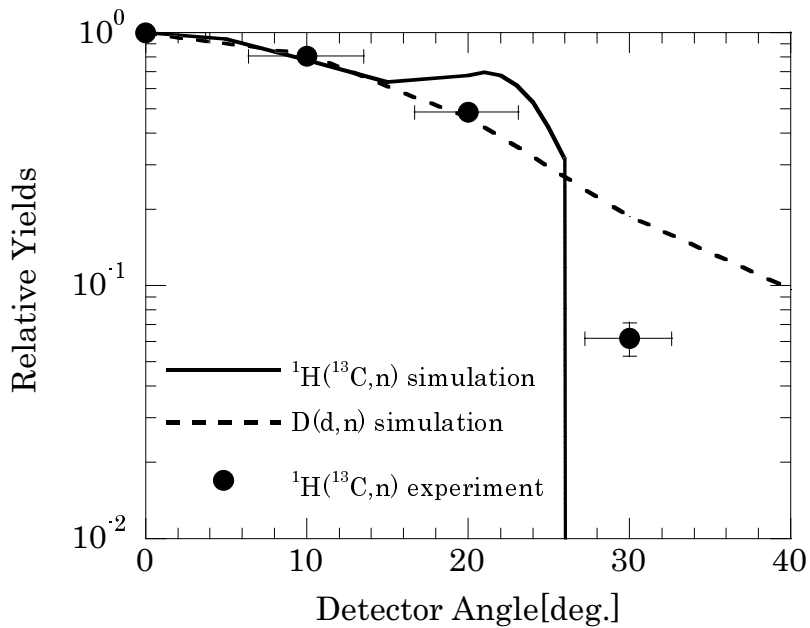


Fig. 7: Angular distributions of neutrons produced by the  ${}^1\text{H}({}^{13}\text{C},\text{n}){}^{13}\text{N}$  reaction. They are normalized to the values at  $0^\circ$ . The solid circles are the experimental data. The solid line is the calculated angular distribution. The dash line represents the calculated angular distribution of neutrons produced by the  $\text{D}(\text{d},\text{n}){}^3\text{He}$  reaction for comparison.